Highly efficient and large-scale generation of functional dopamine neurons from human embryonic stem cells

Myung Soo Cho*†, Young-Eun Lee‡§¶, Ji Young Kim‡§, Seungsoo Chung‡§, Yoon Hee Cho§¶, Dae-Sung Kim‡§, Sang-Moon Kang‡§, Haksup Lee*, Myung-Hwa Kim*, Jeong-Hoon Kim‡§, Joong Woo Leem†‡§, Sun Kyung Oh‖, Young Min Choi‖, Dong-Youn Hwang**, Jin Woo Chang§¶, and Dong-Wook Kim†‡§††‡‡

*Research and Development Center, Jeil Pharmaceutical Co., Ltd., Yongin 449-861, Korea; †Stem Cell Research Center, Seoul 120-752, Korea; ‡Department of Physiology, §Brain Korea 21 Project for Medical Science, ¶Department of Neurosurgery, Yonsei University College of Medicine, Seoul 120-752, Korea; ‖Department of Obstetrics and Gynecology, College of Medicine, Seoul National University, Seoul 110-744, Korea; **CHA Stem Cell Institute, Pochon CHA University College of Medicine, Seoul 135-913, Korea; and ††Center for Cell Therapy, Yonsei University College of Medicine, Seoul 120-752, Korea

Communicated by Sung-Hou Kim, University of California, Berkeley, CA, January 3, 2008 (received for review December 1, 2007)

We developed a method for the efficient generation of functional dopaminergic (DA) neurons from human embryonic stem cells (hESCs) on a large scale. The most unique feature of this method is the generation of homogeneous spherical neural masses (SNMs) from the hESC-derived neural precursors. These SNMs provide several advantages: (*i*) they can be passaged for a long time without losing their differentiation capability into DA neurons; (*ii*) they can be coaxed into DA neurons at much higher efficiency than that from previous reports (86% tyrosine hydroxylase-positive neurons/total neurons); (*iii*) the induction of DA neurons from SNMs only takes 14 days; and (*iv*) no feeder cells are required during differentiation. These advantages allowed us to obtain a large number of DA neurons within a short time period and minimized potential contamination of unwanted cells or pathogens coming from the feeder layer. The highly efficient differentiation may not only enhance the efficacy of the cell therapy but also reduce the potential tumor formation from the undifferentiated residual hESCs. In line with this effect, we have never observed any tumor formation from the transplanted animals used in our study. When grafted into a parkinsonian rat model, the hESC-derived DA neurons elicited clear behavioral recovery in three behavioral tests. In summary, our study paves the way for the large-scale generation of purer and functional DA neurons for future clinical applications.

behavioral recovery | differentiation | Parkinson disease | cell therapy | spherical neural mass

Parkinson's disease (PD) is a neurodegenerative disorder characterized by progressive and selective loss of dopaminergic (DA) neurons in the midbrain substantia nigra (1). Currently, the prevailing strategy for the treatment of PD is pharmacological. However, pharmacological treatment with L-DOPA works initially, but over time, the effectiveness of L-DOPA wanes and side effects develop (2). An alternative approach may be the transplantation of DA-synthesizing cells. One source of DA-synthesizing cells is embryonic stem cells (ESCs). ESCs are pluripotent and capable of self-renewal (3–5). For the purpose of applying the ESCs to PD, many researchers have tried to develop protocols by which ESCs from some species can differentiate into DA neuronal phenotypes (6–11). Although some progress has been made in the generation of DA neurons from human ESCs (hESCs) (12–22), there are still many technical improvements to be made before the application of hESCs to treat PD. Examples include increasing the purity of DA neurons, supplying a sufficient quantity of DA neurons for clinical applications, decreasing tumor formation after transplantation, and clearly demonstrating the functionality of hESC-derived DA neurons in a parkinsonian animal model.

Here, we introduce a method that allows us to differentiate hESCs into functional tyrosine hydroxylase-positive (TH^+) neurons up to near 86% of the total hESC-derived neurons, which is the highest purity ever reported. Achieving high efficiency of DA neuronal derivation is an important issue in cell therapy, because it would not only increase the efficacy of the therapy but also minimize potential disastrous side effects such as teratoma resulting from undifferentiated residual ES cells.

The unique feature of our protocol is the generation of pure spherical neural masses (SNMs). The SNMs can be expanded for long periods without losing their differentiation capability and be coaxed into DA neurons efficiently within a relatively short time (≈2 weeks) when needed. The SNM culture and DA neuron derivation from the SNMs do not need feeder cells, which reduces the risk of contamination of unwanted cells and pathogens. More importantly, our hESC-derived DA neurons induced clear behavioral recovery in three behavioral tests after transplantation in a parkinsonian rat model, indication their functionality *in vivo*; these behavioral data would clarify a recent heated debate about the behavioral recovery by hESC-derived DA neurons in a rat parkinsonian model (14, 23).

Results

Differentiation of hESCs into TH^+ Neurons. In this study, we tried to develop an efficient method for generating DA neurons from hESCs at a high purity and on a large scale. First, detached hESC colonies were cultured on bacterial dishes to form embryoid bodies (EBs) as described in *Experimental Procedures*. For the selection of neural precursors (NPs), the EBs were transferred onto the Matrigel-coated culture dishes and cultured in the presence of 0.5% N_2 supplement for 5 days (Fig. 1, stage 1). The selected NPs then were expanded in the presence of basic FGF (bFGF) and N_2 supplements for 4 days. Most of the selected and expanded NPs expressed nestin and musashi, the markers for NPs (data not shown) (24) and formed neural clumps with neural rosettes (Fig. 1*C*) or neural tube-like morphologies (Fig. 1*D*) (16–17). These neural clumps were isolated mechanically and cultured in suspension on bacterial dishes in the presence of bFGF and N_2 supplements. After approximately 10 days in this culture condition, SNMs

Author contributions: M.S.C. and D.-W.K. designed research; M.S.C., Y.-E.L., J.Y.K., S.C., Y.H.C., D.-S.K., S.-M.K., H.L., and D.-W.K. performed research; J.-H.K., S.K.O., and Y.M.C. contributed new reagents/analytic tools; M.S.C., Y.-E.L., H.L., M.-H.K., J.W.L., D.-Y.H., J.W.C., and D.-W.K. analyzed data; and M.S.C., D.-Y.H., and D.-W.K. wrote the paper.

The authors declare no conflict of interest.

‡‡To whom correspondence should be addressed. E-mail: dwkim2@yuhs.ac.

This article contains supporting information online at www.pnas.org/cgi/content/full/0712359105/DC1.

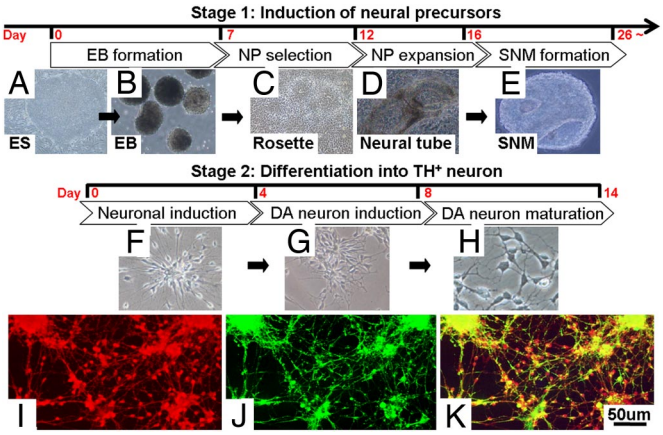

Fig. 1. Differentiation of hESCs into TH$^+$ neurons. Schematic procedures for the *in vitro* differentiation of hESCs. NPs with neural rosettes (*C*) and neural-tube-like structures (*D*) were produced by neural selection and expansion procedures after EB formation (*B*). An SNM (*E*) was then made by using these NPs in a suspension culture (stage 1). After four passages, the SNMs were differentiated into TH$^+$ neurons by treating the cells with signaling molecules, such as SHH, FGF8, and AA (stage 2). The detection of TH$^+$ (*I*) and βIII-tubulin$^+$ cells (*J*) from differentiated hESCs was performed by immunocytochemistry.

that resemble "neurospheres" (25) were formed. For passage, the SNMs were mechanically dissected into ≈4–6 fragments and expanded for ≈7–10 days before the next passage. During the first passage, portions with nonneural morphologies (e.g., cystic structures or spot-forming fibroblast-like cells) were removed by mechanical cutting, increasing the homogeneity of the SNMs. This process was repeated three times (for a total of four passages) to obtain highly homogeneous SNMs. The SNMs could be expanded for at least 120 days, suggesting that our SNM cultures could provide enough number of cells for therapy.

To differentiate the SNMs into neurons, we transferred the SNMs onto Matrigel-coated culture dishes containing differentiation medium (Fig. 1, stage 2). A few days later, cells displayed neuronal morphologies with processes (Fig. 1*F*) and expressed the neuronal markers βIII-tubulin and NeuN (data not shown). To induce TH$^+$ neurons from the cells with neuronal phenotypes, SHH and FGF8 were added into the differentiation medium for 10 days (Fig. 1 *G* and *H*). Cells then were treated with ascorbic acid (AA) for the last 6 days of the 10-day procedure to induce TH$^+$ cell maturation (Fig. 1*H*).

After differentiation into TH$^+$ neurons, immunostaining was performed by using antibodies against TH and βIII-tubulin (Fig. 1 *I–K*). When counted at the cellular level, ≈86 ± 1.4% (≈4–5 × 10^5 cells per 35-mm culture dish) of the βIII-tubulin-expressing cells (total neurons) were TH$^+$ neurons (Fig. 2*A*). Flow cytometry analysis (Fig. 2*B*) revealed that ≈85% of these neurons expressed TH, which is consistent with the cell-counting result. In addition, 77% of the total differentiated cells were βIII-tubulin$^+$ neurons. These results suggest that our protocol could generate TH$^+$ neurons from hESCs much more efficiently than previous protocols (13–18). We also applied our protocol to other hESC lines, such as SNUhES3 and SNUhES16, to confirm that the efficient generation of DA neurons by our protocol is not specific to a certain cell line. After final differentiation, 77.18 ± 1.36% and 81.74 ± 1.52% of the total neurons were TH$^+$ in SNUhES3 and SNUhES16, respectively (Fig. 2 *D–I* and *M*), suggesting that our protocol can be applicable to any hESC line. Interestingly, after 10 passages, the SNMs also retained a similar potential for differentiation into DA neurons (Fig. 2 *J–L*).

The efficiency of DA neuron differentiation also was analyzed at the colony level. This analysis was performed on day 7 during the 14-day differentiation period because individual colonies are hard to distinguish on day 14 of the differentiation procedure. Despite being counted in the middle of differentiation procedure (at day 7), the majority of the colonies (93.38 ± 2.72% from SNUhES1, 91.89 ± 2.48% from SNUhES3, and 92.63 ± 2.43% from SNUhES16) still contained TH$^+$ cells. These numbers also are higher than that from the previous study that demonstrated that 87% of the colonies contained TH$^+$ cells (19).

Characterization of the hESC-Derived TH$^+$ Neurons. We next characterized the subtypes of the hESC-derived TH$^+$ cells because noradrenergic and adrenergic neurons also express TH. To do so, cells were coimmunostained with TH and either En1 (midbrain DA neuron marker), aromatic amino acid decarboxylase (AADC; marker for both catecholaminergic and serotonergic neurons),

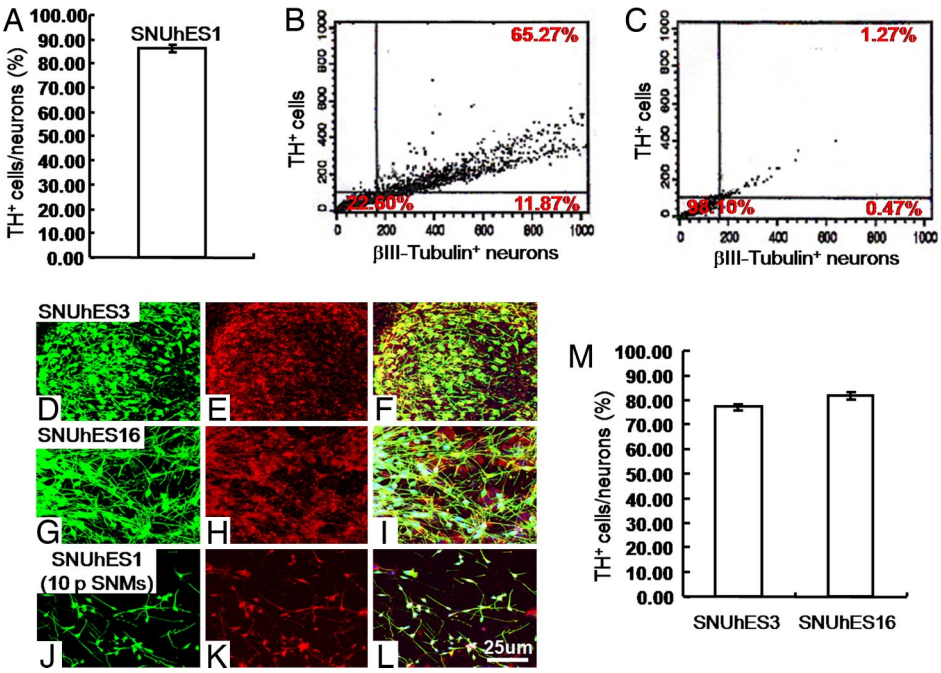

Fig. 2. Quantitative analysis of TH$^+$ and βIII-tubulin$^+$ neurons and the differentiation of TH$^+$ neurons from other hESC lines and highly passaged SNMs. (*A*) The proportion of TH$^+$ neurons to the total number of neurons. TH$^+$ and βIII-tubulin$^+$ neurons (≈15,000 cells from three independent experiments) were counted after performing immunocytochemistry. The value represents the mean ± SEM. (*B* and *C*) Flow cytometric analysis of TH$^+$ and βIII-tubulin$^+$ neurons. Anti-βIII-tubulin and anti-TH antibodies were used for the detection of total neurons and TH$^+$ neurons. Stained cells were analyzed by using a FACScan. This analysis revealed that ≈85% (65.3%/77.1% = 84.7%) of the total neurons were TH$^+$ neurons, and ≈77% of all of the cells were neurons (*B*, sample analysis; *C*, control without primary antibody treatment). (*D–L*) Detection of βIII-tubulin$^+$ (green; *D*, *G*, and *J*) and TH$^+$ (red; *E*, *H*, and *K*) cells after hESC differentiation. SNUhES3 (passage four; *D–F*), SNUhES16 (passage four; *G–I*), and SNUhES1 (highly passaged SNM, passage 10; *J–L*) were used. (*M*) TH$^+$ and βIII-tubulin$^+$ neurons (≈5,000 cells from five independent samples) that were derived from the SNUhES3 and SNUhES16 cell lines were counted after performing immunocytochemistry. The value represents the mean ± SEM.

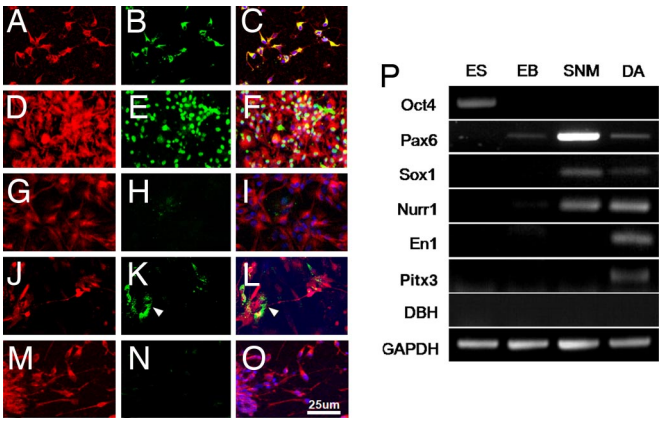

Fig. 3. The majority of TH$^+$ neurons coexpress other markers specific for midbrain DA neurons. The majority of TH$^+$ neurons (*A*, *D*, and *M*) coexpress midbrain DA markers such as AADC (*B*) and En1 (*E*) but not GABA (*N*). Approximately 4% of TH$^+$ (*G* and *J*) cells expressed noradrenergic or adrenergic markers such as DBH (4.18 ± 0.50%; *H*) and PNMT (4.44 ± 0.57%; *K*). ES cell-derived neurons were stained with anti-TH (*A*, *D*, *G*, *J*, and *M*), anti-AADC (DA, serotonergic; *B*), anti-En1 (DA; *E*), anti-GABA (GABAergic; *N*), anti-DBH (noradrenergic and adrenergic; *H*), and anti-PNMT (adrenergic; *K*) antibodies. (*P*) Semiquantitative RT-PCR analysis for neural and DA markers during *in vitro* differentiation of hESCs. The expression levels of each gene were normalized to GAPDH gene expression level. ES, undifferentiated ES cells; EB, embryoid bodies; SNM, spherical neural mass; DA, DA neurons.

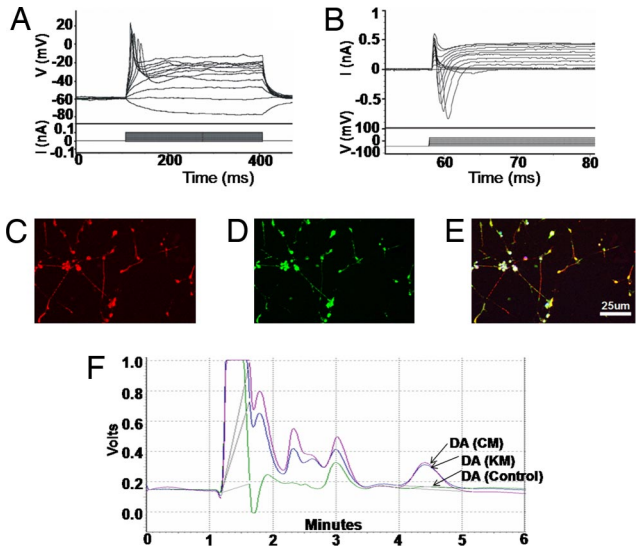

Fig. 4. The hESC-derived DA neurons are biologically functional. (*A* and *B*) Electrophysiological properties of DA neurons differentiated from hESCs. (*A*) Current-clamp recordings during prolonged depolarizing current injections. Bottom traces represent current injections, whereas top traces indicate voltage recordings. The depolarizing current injections elicited fast action potentials. (*B*) Voltage-dependent membrane currents. Depolarizing voltage steps (bottom traces) elicited outward K$^+$ currents and fast inward Na$^+$ currents. (*C–E*) TH$^+$ cells (*C*) coexpress synaptophysin (*D*), which is a protein necessary for synapse formation. Immunostaining was performed by using antibodies against TH and synaptophysin. (*F*) Analyses of dopamine release. DA analysis was performed as described in ref. 27. Results show the HPLC analyses of DA levels in control media (control), 24 h-conditioned media (CM), and 50 mM KCl-challenged media (KM; 30 min) after differentiation.

dopamine β-hydroxylase (DBH; norepinephrine neuron marker), or phenylethanolamine *N*-methyltransferase (PNMT; epinephrine neuron marker) (Fig. 3 *A–L*). Most TH$^+$ cells expressed AADC (Fig. 3 *A–C*), and 91.61 ± 0.64% (≈3.6–4.6 × 10^5 cells per 35-mm culture dish) of the TH$^+$ cells also expressed En1 (Fig. 3 *D–F*). Only a few TH$^+$ cells expressed DBH (4.18 ± 0.50%; Fig. 3 *G–I*) or PNMT (4.44 ± 0.57%; Fig. 3 *J–L*), indicating that the majority of TH$^+$ cells are DA neurons. We noticed that some (≈5%) of PNMT$^+$ cells (Fig. 3*K*) were TH$^-$ and did not have a neuronal morphology. The identity of these cells is yet to be determined. Our hESC-derived TH$^+$ cells also did not express GABA (Fig. 4 *M–O*), therefore indicating that they are not olfactory DA neurons. GFAP and O4, which are markers for astrocyte and oligodendrocyte, respectively, also were not detected (data not shown).

During our procedure for differentiating hESCs to DA neurons, the change of several markers was analyzed by semiquantitative RT-PCR. (Fig. 3*P*). Oct4, a marker for undifferentiated hESCs, was detected only at the ES stage, but not after the initiation of differentiation. At the SNM stage, the NP markers such as Pax6 and Sox1 were strongly up-regulated, and intriguingly, Nurr1, a transcription factor involved in the early specification of DA neurons, already was expressed. At the end of the differentiation procedure, the expression of midbrain DA neuronal markers, such as Nurr1, En1, and Pitx3 were prominent. However, as expected, DBH was hardly detectable. Collectively, the RT-PCR results (Fig. 3*P*) are in line with the immunostaining results (Fig. 3 *A–O*), thus indicating that most of the TH$^+$ neurons generated from our protocol are midbrain DA neurons.

Functional Analyses of DA Neurons. To explore whether the hESC-derived DA neurons were biologically functional, some of the neuronal properties were examined. First, the electrophysiological properties of differentiated neurons were investigated. Recordings in the current-clamp configuration allowed us to determine the active membrane characteristics of these neurons. Prolonged depolarizing current injections demonstrated the capability of the cell to fire fast action potentials and action potential series (Fig. 4*A*). The neurons also exhibited voltage-dependent membrane currents. Depolarizing voltage steps elicited both large outward potassium currents and fast inward Na$^+$ currents (Fig. 4*B*). These results indicate that the differentiated cells have the characteristics of neurons. Additionally, to determine whether these neurons retain normal synapse-forming activity, the differentiated cells were coimmunostained with antibodies against TH and synaptophysin (Fig. 4 *C–E*). Synaptophysin, a membrane glycoprotein of synaptic vesicles that exists in all neurons, is known to be essential for synapse formation and has been widely used as a marker for nerve terminals. As shown in Fig. 4 *C–E*, the TH$^+$ cells expressed synaptophysin, which indicates that the cells have the potential to form synapses (17). An important physiological aspect of the *in vitro* differentiated DA neurons is their ability to produce and release DA in response to membrane depolarization. To test this aspect, hESC-derived DA neurons were analyzed for the production and release of DA. The 24-h conditioned media was prepared at differentiation day 14, and cells then were treated with 50 mM KCl for 30 min. From these samples, DA levels were assayed by reverse-phase HPLC. As shown in Fig. 4*F*, DA released into the conditioned media (24 h) and in response to membrane depolarization (30 min) were 3.24 × 10^{-4} and 3.08 × 10^{-4} pmol per cell, respectively. DA was not detected in the control medium. These results indicate that the neurons derived from hESCs by using our protocol retained the functional properties of DA neurons.

Behavioral Recovery After Transplantation in a Parkinsonian Rat Model. To examine the *in vivo* effect of the hESC-derived DA neurons, we performed several behavioral tests by using a unilaterally lesioned parkinsonian rat model. The PD model was generated by injecting the 6-hydroxydopamine (6-OHDA) into the medial forebrain bundle unilaterally, and the model was validated by an increase in the amphetamine- and apomorphine-induced rotation and a reduction in the forepaw stepping number ("Pre" in Fig. 5). The severity of lesions also was checked by assessing the loss

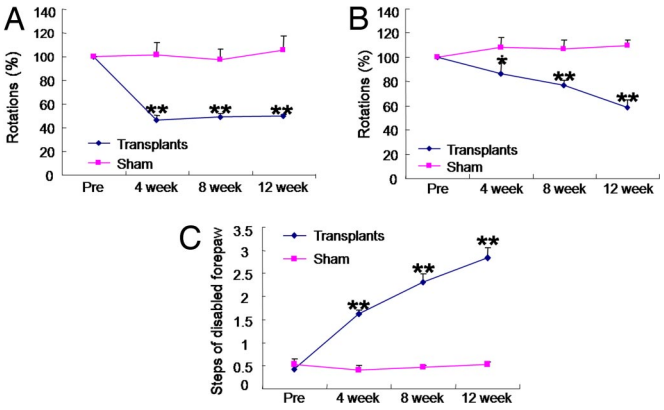

Fig. 5. Behavioral recovery by hESC-derived neurons in a parkinsonian rat model. The behavior of PD animals grafted with neurons differentiated from SNUhES1 and sham controls was tested before transplantation (Pre) and at 4, 8, and 12 weeks after the grafting. (*A*) Apomorphine-induced rotation response per hour (three independent experiments until 12 weeks, $n = 6$). (*B*) Amphetamine-induced rotation response per hour (three independent experiments until 12 weeks, $n = 6$). Only rats that showed a significant turning behavior (>310 turns per hour) after drug administration were used in our study. The rotational scores (rotation %) in *A* and *B* are expressed as a percentage of rotations compared with the values obtained from the Pre time point. *, significantly different from sham controls at $P < 0.01$; **, $P < 0.001$. (*C*) The adjusting step test is expressed as the number of steps per 0.9 m on a treadmill (at a rate of 0.075 m/s) with the disabled forepaw (four independent experiments until 12 weeks, $n = 14$).

of TH^+ fibers and cell bodies in the striatum and the substantia nigra, respectively (Fig. 6*A*). Three weeks after the 6-OHDA lesion was generated, $\approx 5 \times 10^5$ differentiated neurons that had been collected on day 7 of the 14-day differentiation procedure (Fig. 1, stage 2) were introduced into the striatum of the lesioned side. The effects of the grafted cells on behavioral recovery were evaluated at the 4th, 8th, and 12th weeks after transplantation by three behavioral tests: the apomorphine-induced rotation test (Fig. 5*A*), the amphetamine-induced rotation test (Fig. 5*B*), and the forepaw step-adjusting test (Fig. 5*C*).

We first evaluated behavioral recovery by drug-induced rotation tests. Apomorphine and amphetamine administration into the PD model induced a movement bias that was contralateral and ipsilateral, respectively, to the lesioned side (Fig. 5 *A* and *B*). In both cases, sham control PD animals maintained a consistently high number of rotations until the last time point measured (12 weeks posttransplantation). On the contrary, the PD animals grafted with the hESC-derived cells showed a significant reduction in rotational scores. Apomorphine-induced rotation went down to 49.43 ± 1.74% ($n = 6$) of the original level (the level before transplantation, marked "Pre" in the *x* axis) at 12 weeks posttransplantation (Fig. 5*A*). Twelve weeks after the engraftment, amphetamine-induced rotation was reduced down to 58.37 ± 5.9% ($n = 6$) of the levels observed before transplantation (Fig. 5*B*). In normal rats, the scores were very low (ipsilateral rotation number: ≈18.5/h; contralateral rotation number: ≈11/h). Intriguingly, the pattern of the rotation reduction was different between the two drug-induced tests. The apomorphine-induced rotation number was rapidly reduced, reaching a minimal level at 4 weeks after transplantation, and the reduced level was maintained until the 12-week time point (Fig. 5*A*). In contrast, the amphetamine-induced rotation was gradually reduced over time during the 12 weeks posttransplantation period (Fig. 5*B*).

The forepaw-adjusting step test reflects a more direct measure of motor deficit because it is a nonpharmacological test. As shown in Fig. 5*C*, a sham control PD group showed almost no stepping of the disabled forepaw (contralateral to the lesioned side) throughout the 12-week period. However, the PD animals grafted with hESC-derived cells showed a significant improvement in stepping number over time during the 12-week period (four independent experiments, $n = 14$).

Histological Analyses of the Grafts. Twelve weeks after engraftment, the rats were killed and then analyzed for the survival of transplanted hESC-derived cells with human-specific antibodies (Fig. 6). A total number of 395,671 ± 150,378 cells per rat ($n = 6$, 180,672 cells per mm^3, average graft size: 2.18 ± 0.76 mm^3) had survived around the injection area and were stained with antibodies against either human nuclei or mitochondria-specific antigen (Fig. 6). Most of the hESC-derived cells expressed the neuronal marker βIII-tubulin (Fig. 6*B*). We next examined the presence of hESC-derived TH^+ cells. In the grafts, we were able to detect TH^+ cells that were costained with antibody against human nuclei (Fig. 6*C*). The number of TH^+ cells were 10,732 ± 4,132 cells per rat (2.7% of the

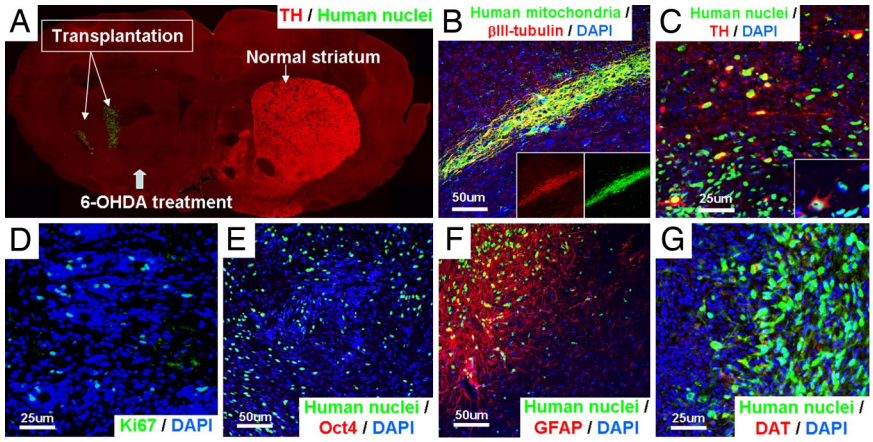

Fig. 6. Characterization and survival of the transplanted cells in a parkinsonian rat model. (*A*) Tiled coronal sections of the rat brain showing the 6-OHDA-treated side (*Left*) and the cells in the injection area (human nuclei, green). The normal striatum was stained with anti-TH antibody (red). (*B*) The human cells (human mitochondria, green) are predominantly βIII-tubulin$^+$ (red), indicating that most of the human cells are neurons. (*C*) Twelve weeks after transplantation, survival of TH^+ cells was analyzed by immunohistochemistry using anti-human nuclei antibody (green) and anti-TH antibody (red). The TH^+ cells colocalized with human marker. (*D*) $Ki67^+$ cells (green) were found in the grafted region, indicating the existence of proliferating cells. (*E*) $Oct4^+$ cells were not detected. (*F*) Association of grafted cells and astrocytes was confirmed by immunostaining using anti-human nuclei (green) and anti-GFAP (red) antibodies. (*G*) Immunostaining of DAT (red) to confirm the maturity of the grafted DA neurons; human nuclei (green).

surviving hESC-derived cells, 4,901 cells per mm^3). Although some proliferating ($Ki67^+$) cells (<3%) were found in the grafted area (Fig. 6*D*), the cells expressing markers for undifferentiated hESCs such as Oct 4 (Fig. 6*E*) were not detected in the grafts. We also have not detected teratoma formation from any animals grafted with hESC-derived cells. Interestingly, endogenous astrocytes were located very close to the hESC-derived cells (Fig. 6*F*). We observed only a small portion of the TH^+ neurons are expressing dopamine transporter (DAT), suggesting that many TH^+ neurons are not fully matured yet at 12 weeks posttransplantation (Fig. 6*G*).

Discussion

Efficient and large-scale generation of DA neurons from hESCs is a very important challenge for designing a cell-replacement therapy procedure for PD. In addition, one of the current controversial issues is a clear demonstration of the functionality of hESC-derived DA neurons in an animal model of PD. Although several protocols for the differentiation of hESCs into DA neurons have been reported (12–22, 26), protocols with more advantages, such as those that yield a high purity of DA neuron pool, show clear *in vivo* functionality, lack the requirement for feeder cells, supply ample quantity of DA neurons, and allow for a relatively fast differentiation, are still to be developed to bring hESC-mediated cell therapy closer to reality.

Previous protocols generate DA neurons from neural rosettes grown attached on Matrigel. In contrast, we generate DA neurons from SNMs that have been expanded as spheres.

Several unique procedural advantages are associated with these SNMs. First, the hESC-derived SNMs can be coaxed into DA neurons at the highest efficiency reported to date. Our results shows that 77% of our cultures are neurons and 86% of the neurons are DA neurons, indicating that ≈66% of the total cells are DA neurons. These values are much higher than those in the previous reports (i.e., <40% of total cells were reported to be TH^+ neurons) (12–18). Second, the SNMs can be expandable for a long time (at least 4 months), while maintaining the same phenotype and capability to differentiate into DA neurons (Fig. 2 *J–L*). According to our estimation, $\approx 1.72 \times 10^7$ TH^+ cells could be produced from the four time-passaged SNMs originated from a single undifferentiated hESC colony. The expandability of SNMs would allow us to provide a sufficient amount of DA neurons for future clinical applications. Third, the expanded SNMs can be stored frozen and thawed at any time. Fourth, the generation of DA neurons from SNMs takes a relatively short time (≈2 weeks). Finally, feeder cells are not used in the SNM expansion and differentiation, which would save a lot of time and effort required for handling feeder cells and reduce the risk of contamination from irrelevant cells during transplantation.

Mechanical handling of the SNMs for passaging might need some effort. However, in our experience ≈100 SNMs per hour could be passaged by mechanical manipulation and $\approx 1.2 \times 10^5$ TH^+ cells could be obtained from a single SNM after differentiation. This mechanical work cannot be replaced by enzymatic digestion with collagenase, trypsin, and accutase because the survival rate of the cells becomes very low and the purification process of the SNMs (removal of nonneural cells) cannot be achieved.

According to the immunocytochemistry and RT-PCR analyses, the majority of the TH^+ neurons obtained from our protocol have the DA neuronal phenotype (Fig. 3). Only 4–5% of the TH^+ cells were noradrenergic or adrenergic neurons (Fig. 3 *G–L*). GFAP and O4-expressing cells were hardly detectable, indicating that no glial cells were generated by the protocol (data not shown).

To determine whether the hESC-derived DA neurons could reverse the behavioral deficits seen in a parkinsonian rat model, we attempted to transplant the hESC-derived cells into the striatum of the lesioned side of the PD model. According to our experience, the stage of the cells during differentiation process, the condition of the cells, and several other parameters are critical for a successful transplantation study (11, 27). For example, if much less differentiated cells are used, teratoma formation may occur; however, if fully differentiated cells are transplanted, the survival rate is too low. In this study, we transplanted the cells on day 7 of the 14-day differentiation procedure. At this stage, the TH gene was beginning to be expressed (≈50% of the neurons are TH^+; data not shown), suggesting that these cells are being committed to DA neuronal lineage and/or are at the initial stage of DA neuronal specification. After injecting 500,000 cells into the striatum on the lesioned side, we analyzed the number of surviving cells at 12 weeks posttransplantation. Histochemical analyses showed that 395,671 ± 150,378 cells were surviving, and most of the grafted cells were neurons. We also found that 10,732 ± 4,132 cells (2.7% of the surviving human cells) were TH^+. In contrast to the *in vitro* result, not many TH^+ cells were detected in the grafts. It is thought that two reasons are responsible for this. First, DA neurons may be more susceptible than other neurons to various environmental insults and stresses. Therefore, it is possible that DA neurons were preferentially lost during/after transplantation. Second, SNM-derived cells were transplanted on day 7 of the 14-day differentiation procedure. At this time point, some cells still may not committed to the DA neuron lineage, forming other types of neurons after transplantation. Histological analysis revealed that a small number of $5\text{-}HT^+$ serotonergic neurons (<1%) were detected and no GABAergic neurons ($GABA^+$) were detected. Oligodendrocytes also were not detected in the grafts [supporting information (SI) Fig. 7].

Oct4-expressing cells were not detected, although a few $Ki67^+$ cells (<3%) were present (Fig. 6 *D* and *E*). These data suggest that grafted cells did not contain undifferentiated ES cells and, in line with this observation, no teratomas were found in any of the engrafted animals used in our study.

A successful and clear behavioral recovery has not been reported in an animal model of PD using DA cells or DA precursor cells derived from hESCs. One research group reported a partial behavioral deficit recovery by using uncommitted hESC-derived NPs (not DA neuronal precursors) in a PD rat model. However, only 0.18 ± 0.05% of the engrafted cells were found to become TH^+ neurons, thus explaining the partial behavioral recovery that they observed (26). Very recently, Roy *et al.* (14) reported that hESC-derived DA neurons generated by coculture with immortalized midbrain astrocytes brought about behavioral recovery in an apomorphine-induced rotation test and the adjusting stepping test of a PD rat model. However, as stated in a recent correspondence (23), several questions and concerns were raised about the functionality of the engraftment in their behavioral tests. These concerns were over the possibility of nonspecific graft effects in their apomorphine-induced turning test, misinterpretation of the adjusting step test, and a lack of clear validation of the animal model used.

In our study, we used a standard method to generate a unilateral rat model (injection of 6-OHDA into the medial forebrain bundle) and confirmed the level of the ipsilateral lesion by drugs (both apomorphine and amphetamine)-induced rotation and histological analyses (Figs. 5 and 6). Only animals that showed a significant turning behavior (>310 turns per hour) after drug administration were selected for our behavioral study. Compared with sham control, our cell engraftment-induced behavioral recovery was prominent in all three tested behavioral assessments: apomorphine-induced rotation, amphetamine-induced rotation, and forepaw-stepping tests (Fig. 5). Interestingly, the apomorphine-induced rotation was reduced to a minimum level as early as 4 weeks posttransplantation (Fig. 5*A*). Because we cannot rule out the possibility that this result may reflect a nonspecific effect of the graft, as Christophersen and Brundin pointed out in their correspondence (23), we tried the amphetamine-induced rotation and forepaw-adjusting step tests. These tests are known to be better indicators of the effect of the DA that is produced from the surviving grafts than the apomorphine-induced rotation test (28, 29). Amphetamine-induced rotation was reduced over time during the 12-week period posttransplantation (Fig. 5*B*). The forepaw-

adjusting test (Fig. 5*C*) also clearly demonstrates that the disabled paw contralateral to the lesioned side of the brain was recovered by the grafts at the lesioned striatum, as judged by the increase in the number of steps taken. The results from the amphetamine-induced rotation and the forepaw-adjusting step tests evidently demonstrate that our hESC-derived DA neurons bring about behavioral recovery in a rat model of PD. Although we observed clear behavioral recoveries in three tests we tried, we have not detected any contralateral rotation after amphetamine treatment. One possible reason might be that many TH^+ neurons are still in immature status and are on the way to full maturation at the last time point we performed the behavioral measurement (12 weeks after transplantation). This interpretation was supported by the fact that only a portion of the TH^+ neurons were DAT^+ (Fig. 6*G*). Furthermore, in line with this interpretation, we have observed that the number of amphetamine-induced turn was further decreased at 14 weeks after transplantation (data not shown).

In conclusion, we developed an efficient protocol that can generate functional DA neurons from hESCs at the highest yield ever reported and, importantly, the differentiation procedure was carried out without any genetic modification or coculture with feeder cells, increasing safety after transplantation. In a parkinsonian animal model, these neurons were able to reverse the motor deficits in all three tests commonly used to measure the efficacy of PD therapeutic regimens. Our work also provides a method of producing a large number of DA neurons through SNM expansion, which might be a critical issue for future clinical applications. We strongly believe that our study sets a firm stage for the development of efficient therapeutic regimens for future cell-replacement therapy in the treatment of PD.

Experimental Procedures

Differentiation of hESCs into DA Neurons. The undifferentiated hESC lines SNUhES1, SNUhES3, and SNUhES16 were maintained as described in ref. 30. For differentiation, hESC colonies were detached and were cultured in a bacterial dish for 7 days to form EBs. EBs then were cultured in NP selection media for 5 days, and the resulting NPs were expanded for another 4 days in an expansion medium (see *SI Text*). To form SNMs, neural rosettes and neural tube-like structures that were observed during neural expansion culture were mechanically isolated and cultured onto bacterial culture dishes containing the NP expansion medium. For passaging, the SNMs were mechanically fragmented into four to six pieces and expanded for ≈7–10 days. Homogeneous SNMs generated by a mechanical purification process during the first four passages can be expanded for an extensive time (>4 months). These pure SNMs were used for differentiation into DA neurons (see *SI Text*).

Immunostaining and Flow Cytometry Analysis. Immunostaining was performed as described in ref. 11 (see *SI Text*). For flow cytometry analysis, cells were dissociated by incubation for 5 min in 0.05% trypsin/0.1% EDTA (Invitrogen) at 37°C and then incubated in perforation solution (0.05% Triton X-100) for 5 min. After the antibody treatment, cells were analyzed by using FACScan and CellQuest Pro software (BD Bioscience).

RT-PCR. RT-PCR was performed as described in ref. 11. Primer sequences and the length of the amplified products are described in *SI Text*.

Production of a Parkinsonian Rat Model, Cell Transplantation, and Behavioral Testing. Male Sprague–Dawley rats weighing 200–230 g were used to generate parkinsonian rat models. Experimental groups were divided into three groups: (*i*) a normal group without lesions, (*ii*) a sham control group with 6-OHDA lesions, and (*iii*) a group with 6-OHDA lesions that were transplanted with neurons derived from hESCs. The detailed surgical procedures are described in the *SI Text*.

Two weeks after the development of 6-OHDA-induced lesions, the animals were tested for amphetamine-induced (3 mg/kg i.p.) and apomorphine-induced (0.1 mg/kg i.p. in saline containing AA at 2 mg/ml; Sigma) turning behavior and forepaw-adjusting stepping, as described in ref. 27. Each forepaw-adjusting step test consisted of five trials for the disabled forepaw.

One week after behavioral testing, hESC-derived neurons were transplanted into the ipsilateral striatum (see *SI Text*). Behavioral testing was conducted after the 4th, 8th, and 12th week posttransplantation.

ACKNOWLEDGMENTS. This work was supported by Grants SC1020, SC4001, and SC2160 from the Stem Cell Research Center of the 21st Century Frontier Research Program funded by the Ministry of Science and Technology, Republic of Korea.

1. Youdim MB, Riederer P (1997) Understanding Parkinson's disease. *Sci Am* 276(1):52–59.
2. Olanow CW, Obeso JA (2000) Levodopa motor complications in Parkinson's disease. *Ann Neurol* 47:167–178.
3. Evans MJ, Kaufman MH (1981) Establishment in culture of pluripotential cells from mouse embryos. *Nature* 292:154–156.
4. Desbaillets I, Ziegler U, Groscurth P, Gassmann M (2000) Embryoid bodies: An in vitro model of mouse embryogenesis. *Exp Physiol* 85:645–651.
5. Wichterle H, Lieberam I, Porter JA, Jessell TM (2002) Directed differentiation of embryonic stem cells into motor neurons. *Cell* 110:385–397.
6. Lee SH, Lumelsky N, Studer L (2000) Efficient generation of midbrain and hindbrain neurons from mouse embryonic stem cells. *Nat Biotechnol* 18:675–679.
7. Kawasaki H, *et al*. (2000) Induction of midbrain dopaminergic neurons from ES cells by stromal cell-derived inducing activity. *Neuron* 28:31–40.
8. Kim JH, *et al*. (2002) Dopamine neurons derived from embryonic stem cells function in an animal model of Parkinson's disease. *Nature* 418:50–56.
9. Chung S, *et al*. (2002) Genetic engineering of mouse embryonic stem cells by Nurr1 enhances differentiation and maturation into dopaminergic neurons. *Eur J Neurosci* 16:1829–1838.
10. Takagi Y, *et al*. (2005) Dopaminergic neurons generated from monkey embryonic stem cells function in a Parkinson primate model. *J Clin Invest* 115:102–109.
11. Kim DW, *et al*. (2006) Stromal cell-derived inducing activity, Nurr1, and signaling molecules synergistically induce dopaminergic neurons from mouse embryonic stem cells. *Stem Cells* 24:557–567.
12. Sonntag KC, Pruszak J, Yoshizaki T, van Arensbergen J, Sanchez-Pernaute R, Isacson O (2007) Enhanced yield of neuroepithelial precursors and midbrain-like dopaminergic neurons from human embryonic stem cells using the bone morphogenic protein antagonist noggin. *Stem Cells* 25:411–418.
13. Brederlau A, *et al*. (2006) Transplantation of human embryonic stem cell-derived cells to a rat model of Parkinson's disease: Effect of in vitro differentiation on graft survival and teratoma formation. *Stem Cells* 24:1433–1440.
14. Roy NS, Cleren C, Singh SK, Yang L, Beal MF, Goldman SA (2006) Functional engraft of human ES cell-derived dopaminergic neurons enriched by coculture with telomerase-immortalized midbrain astrocytes. *Nat Med* 12:1259–1268.
15. Ueno M, *et al*. (2006) Neural conversion of ES cells by an inductive activity on human amniotic membrane matrix. *Proc Natl Acad Sci USA* 103:9554–9559.
16. Park CH, *et al*. (2005) In vitro and in vivo analyses of human embryonic stem cell-derived dopamine neurons. *J Neurochem* 92:1265–1276.
17. Yan Y, *et al*. (2005) Directed differentiation of dopaminergic neuronal subtypes from human embryonic stem cells. *Stem Cells* 23:781–790.
18. Perrier AL, *et al*. (2004) Derivation of midbrain dopamine neurons from human embryonic stem cells. *Proc Natl Acad Sci USA* 101:12543–12548.
19. Zeng X, *et al*. (2004) Dopaminergic differentiation of human embryonic stem cells. *Stem Cells* 22:925–940.
20. Schulz TC, *et al*. (2004) Differentiation of human embryonic stem cells to dopaminergic neurons in serum-free suspension culture. *Stem Cells* 22:1218–1238.
21. Park S, *et al*. (2004) Generation of dopaminergic neurons in vitro from human embryonic stem cells treated with neurotrophic factors. *Neurosci Lett* 359:99–103.
22. Buytaert-Hoefen KA, Alvarez E, Freed CR (2004) Generation of tyrosine hydroxylase positive neurons from human embryonic stem cells after coculture with cellular substrates and exposure to GDNF. *Stem Cells* 22:669–674.
23. Christophersen NS, Brundin P (2007) Large stem cell grafts could lead to erroneous interpretations of behavioral results? *Nat Med* 13:118.
24. Zhang SC, Wernig M, Duncan ID, Brustle O, Thomson JA (2001) In vitro differentiation of transplantable neural precursors from human embryonic stem cells. *Nat Biotechnol* 19:1129–1133.
25. Reynolds BA, Weiss S (1992) Generation of neurons and astrocytes from isolated cells of the adult mammalian central nervous system. *Science* 255:1707–1710.
26. Ben-Hur T, *et al*. (2004) Transplantation of human embryonic stem cell-derived neural progenitors improves behavioral deficit in Parkinsonian rats. *Stem Cells* 22:1246–1255.
27. Cho YH, *et al*. (2006) Dopamine neurons derived from embryonic stem cells efficiently induce behavioral recovery in a Parkinsonian rat model. *Biochem Biophys Res Commun* 341:6–12.
28. Curran EJ, Albin RL, Becker JB (1993) Adrenal medulla grafts in the hemiparkinsonian rat: Profile of behavioral recovery predicts restoration of the symmetry between the two striata in measures of pre- and postsynaptic dopamine function. *J Neurosci* 13:3864–3877.
29. Chang JW, Wachtel SR, Young D, Kang UJ (1999) Biochemical and anatomical characterization of forepaw adjusting steps in rat models of Parkinson's disease: Studies on medial forebrain bundle and striatal lesions. *Neuroscience* 88:617–628.
30. Oh SK, *et al*. (2005) Derivation and characterization of new human embryonic stem cell lines, SNUhES1, SNUhES2 and SNUhES3. *Stem Cells* 23:211–219.